

# Analysis of the temperature-induced structural static properties of a long-span steel box-girder suspension bridge

Linren Zhou<sup>1</sup>, Lan Chen<sup>1</sup>, Yong Xia<sup>2</sup> and Ki Young Koo<sup>3</sup>

<sup>1</sup>School of Civil and Transportation Engineering, South China University of Technology, Guangzhou, China

<sup>2</sup>Department of Civil and Environmental Engineering, The Hong Kong Polytechnic University, Hong Kong, China

<sup>3</sup>College of Engineering, Mathematics and Physical Sciences, University of Exeter, Exeter, United Kingdom

Temperature is one of the most significant and negative environmental effects on bridge, even worse for long-span steel box-girder bridge. In this study, the temperature-induced (T-I) static responses of a long-span suspension bridge under real service environmental conditions are investigated using numerical simulation and field measurement. The fine 2-D finite element (FE) models of a typical section for box-girder, main cable, hanger, tower column and cross beam are constructed. The thermal boundary conditions are determined strictly according to the surrounding environments of a sunny day and applied on the FE models, then transient heat-transfer analysis is performed to obtain the time-dependent temperature and distribution of the bridge. A fine 3-D FE model of the entire bridge for structural analysis also is particularly developed in term of the real conditions. The calculated temperatures are correspondingly applied on the 3-D FE model and T-I structural responses can be simulated. The bridge static responses caused by design vehicle load are also calculated for comparison. The simulated temperatures and T-I static responses have good agreement with the measured counterparts, which verify the numerical simulation method. The main cable and bridge deck make the main contributions to the temperature effects of suspension bridge. Comparing to the static responses of design vehicle load, the diurnal variation of T-I static responses are considerable, even large than those of the design vehicle load.

**Keywords:** Long-span suspension bridge; Temperature effects; Static response; Design vehicle load; Field monitoring

## 1. Introduction

Bridges, particularly large and long-span bridges in seaside environment, have a long service life and suffering harsh environments. The harsh service environments degenerate the performance of bridges even lead to catastrophic collapse. Temperature effect has been widely recognized as one of the most significant and negative effects on bridge. The variation of bridge temperature and distribution caused by the changes of surrounding meteorological

environments, subsequently affect the structural static and dynamic properties and result in structural responses such as movement, deformation, stress, crack, reaction, and change of connection and boundary condition. Actually, many studies and field measurements indicated the temperature-induced (T-I) responses were even more large than these of the external operational loads (Priestley, 1976; Priestley, 1978; Kennedy, 1987; Salawu, 1997). The negative temperature effects cost a considerable fraction of the carrying capacity and degenerate the performance of bridges, they are key issues in the entire life-cycle of bridge, and should be seriously considered for bridge design, construction and operating maintenance.

Bridge temperature effect has attracted attention as an engineering issue and been investigated since 1960s (Zuk, 1965). The analysis of temperature effect on bridge mainly includes two parts: structural temperature and the T-I response. Obtaining the time-dependent structural temperature and distribution is the fundament for temperature effect analysis. The field monitoring is the most intuitive way and driven the investigation of bridge temperature effect at the very beginning (Priestley, 1976; Priestley, 1978; Kennedy, 1987) . The measurements can be directly used for analysis and mathematical expressions can then be derived. There is a vast literature on investigating bridge temperature effects using data-driven approaches based on field measurements (Římal, 2001; Roberts-Wollman, et al., 2002; Kromanis and Kripakaran, 2017; Zhou, et al., 2018; Zhou and Sun, 2019) . Field monitoring is possible for large and long-span bridges since a SHM system always be installed. However, the limited measuring points cannot fully and precisely capture the temperature distribution of the entire bridge. Besides, the in-situ monitoring is infeasible for all normal bridges because of high cost and time-consuming. Numerical method can provide a high efficiency and low-cost approach to calculate the structural temperature and T-I response. The structural temperature assumed to be one-dimensional (1-D) and linear distribution were firstly investigated. (Emerson, 1973; Kehlbeck, 1975; Hunt, 1975). The 1-D linear models are difficult to reasonably express the temperature distribution of large and complex bridges such as box girder bridge, therefore, two-dimensional (2-D) methods were developed (Elbadry, 1983; Tong, 2001). However, 2-D method can't achieve desirable accuracy for large bridge with complex configuration and long-span. With the rapid development of computer technique and higher demands for structural analysis, the numerical simulation method using large commercial finite element (FE) software is widely adopted. It can provide comprehensive and high accuracy of fine analysis for temperature behavior of bridges, especially for the large and long-span bridges. (Xia, 2013; Zhou, et al., 2015; Tayşi and Abid, 2015; Zhu and Meng, 2017).

Temperature is a major environmental action on bridge(Zhou and Yi, 2013).The variation of temperature and distribution will change the bridge geometrical and material properties as well as boundary conditions, subsequently generate the structural responses of static and dynamic. The T-I responses are high depended on the bridge type and

structural material. Normally, more significant temperature effects are observed on large and long-span bridges such as long-span cable-stayed bridge and suspension bridge, and the box-girder and steel material make these even worse (Xu, et al., 2010; Xia, et al., 2013; Tomé, et al., 2018; Yang, et al., 2018; Westgate, et al., 2014). The T-I stress and displacement (or movement) of bridge were widely measured and investigated since 1970s. (Reynolds, 1972; Emerson, 1979; Dilger, et al., 1983; Mirambell and Aguado, 1990; Moorty and Roeder, 1992). Fujino, et al. (Fujino, et al., 2000) pointed out the temperature constituted the major factor affecting their configurations of long-span suspension bridges. Yang, et al. (2010) conducted field monitoring on a long-span suspension bridge, the annual change of the displacement at the end of bridge girder was larger than half a meter. Kromanis, et al. (2016) found significant T-I displacements and forces imposed at the bearings of a seven-span steel box-girder bridge, which remarkably larger than the vehicle load responses.

It is very important to assess the temperature effects and ensure the safety of bridge. The bridge T-I static responses are considerable and relatively easy to be collected with desirable reliability and accuracy, many assessment and design methods for bridge temperature effects were proposed and investigated based on T-I static responses. Roeder (2003) proposed a design method for expansion joints to accommodate T-I movements of different bridge types, the method was compared with existing AASHTO Specifications and field observations. Ni, et al. (2007) provided an approach to evaluate the conditions of bridge expansion joints using long-term field measurements of movement and temperature. Duan, et al. (2011) investigated the correlation between strain and temperature of a tied arch bridge, and quantify the temperature effects based on measurements of strain response. Wang, et al. (2015) conducted an assessment of a steel truss arch girder bridge, it found the changes of static strain mainly caused by temperature variation and the T-I strain shown apparent linear correlation with the temperature. Xia, et al. (2016) presented a new method for damage identification using measured T-I strain of a long-span suspension bridge and then evaluated the bridge conditions.

Obviously, the structural temperature is a kind of load action on bridge, such as vehicle, wind and seismic action. However, the temperature effect is a very slow variation in diurnal periodic, it is invisible and hard to be perceived in an instant. The temperature effect will lead to damages, age the material, reduce the carrying capacity and degrade the bridge performance. Very component of bridge at very moment, the temperature effects are existing. However, it seems never a bridge failure or collapse directly due to temperature effects, which give rise to one of the most significant current discussions about temperature effects is how actually severe of this kind of negative impact on bridge. To partly clarify this issue, in this study, the T-I static responses of a long-span steel box-girder suspension bridge are investigated using numerical simulation and field monitoring. This paper is organized as follows:

1. The long-span suspension bridge and the installed SHM system are briefly introduced.
2. The fine FE models for thermal analyses and structural analysis are constructed.
3. The structural temperatures of entire bridge on a sunny day are calculated and compared with the measurements to validate the numerical model and methodology.
4. The T-I static responses of suspension bridge are calculated and the results are compared and discussed with the counterparts of measurements and simulations of design vehicle load.
5. Conclusions and suggestions are drawn for T-I static responses of long-span box-girder suspension bridge.

## 2. Engineering background

### 2.1 Humber Bridge

The Humber Bridge is located at the estuary of the river Humber, England. It was began constructing in March 1973 and opened to traffic on 24 June, 1981. The main bridge of Humber Bridge is total length 2220 m with an asymmetry layout 280m (north) + 1410m + 530m (south), as shown in Fig. 1. The 1410m main span was the longest suspension bridge in the world for 17 years since its inauguration, and now it is the seventh-longest of its type in the world(Hyder, 2007).

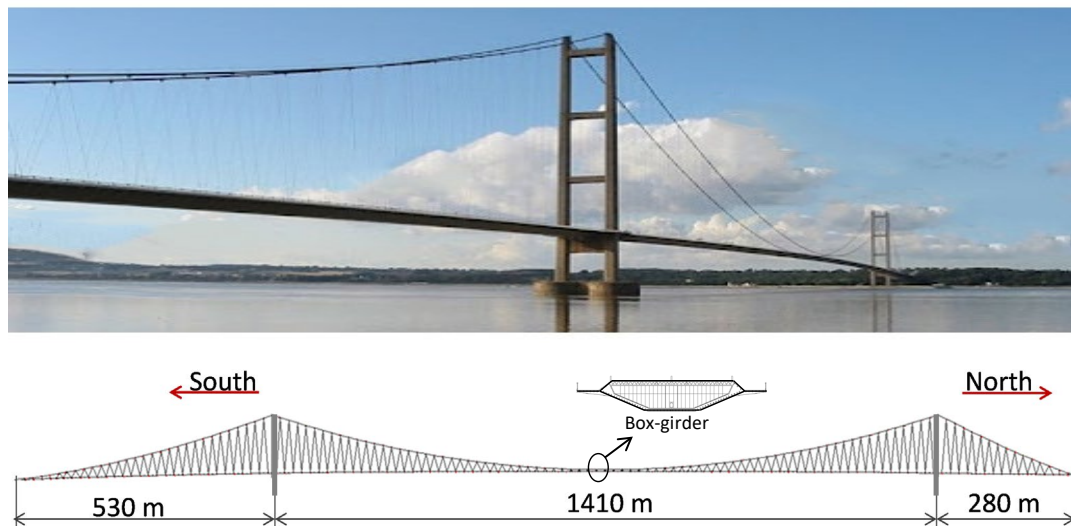


Fig. 1. Humber Bridge

The bridge carries a dual two-lane highway, footpaths and cycle tracks. The steel box-girder was design to be a

streamlined hollow box with 4.8 m height and 18 m wide upper surface, which covered with 41 mm thickness rubberized bitumen asphalt. Two flanges with width of 3 m along each side of the boxes cantilever outwards to carry the footpaths and cycle tracks. The north tower is located at the shore and the south tower is located in the water 500 m from the shore line. Tower height above piers is 155.5 m. Each tower has two hollow-section columns connected by four cross beams, as shown in Fig. 1. The top and bottom cross beams are hollow-section. The main cables were designed for a maximum pull of 19,400 tonnes and each cable consists of 14,948 parallel galvanized drawn wires of 5 mm diameter. Since the bridge is asymmetry, the suspension cable at the north side span with relative steep slope is consequent greater tension. Therefore, there are an additional 800 wires fixed to the main anchorage and the tower saddles(Fisher, 1982).

## 2.2 SHM system of Humber Bridge

A Structural Health Monitoring (SHM) system has been installed on the bridge, and collected a large amount of field data since 2011. The SHM system mainly includes three subsystems: sensor system, network system and data management system. The sensor system can be generally divided into four parts according to the sensing characteristics. 1) Meteorological parameters: the field air temperature, wind speed and wind direction. 2) Dynamics responses: accelerometers at the mid-span for vibration monitoring. 3) Static responses: four extensometers were installed for each columns of towers. An inclinometer at the mid-span for lateral inclination of bridge deck. Two GPS were fixed on the suspension cables at the mid-span of bridge. 4) Structural temperature: six thermocouples monitoring the temperature of the box girder section at the mid-span, as shown in Fig. 2. Two temperature sensors were installed at the middle of left lane of northbound carriageway to collect the surface temperature of the asphalt and ground temperature on the interface between steel surface and paved asphalt; four temperature sensors were placed on the top, bottom, east and west of inside surface of box girder, respectively.

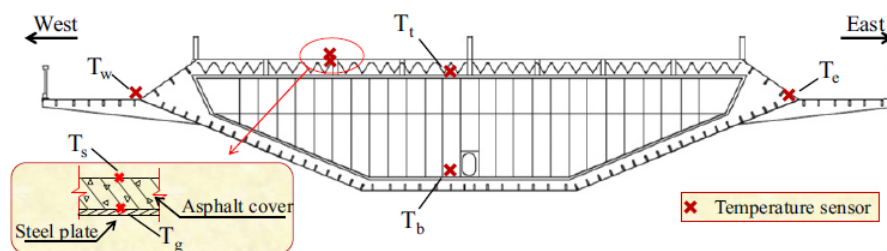


Fig. 2. Arrangement of temperature sensors in the box girder section at mid-span

### 3. Finite element Models

#### 3.1 FE model for thermal analysis

For slender structural components, the section temperatures along the long direction are assumed to be constant. Therefore, the temperature of box-girder, suspension cable, hanger, tower column and cross beam can be calculated using 2-D section element model. In this study, the FE models for temperature analysis of are established using ANSYS software package. The FE models of the typical section of the box girder, suspension cables, hangers and bridge towers of this suspension are constructed for thermal analysis, as shown in Fig. 3. All the FE models are developed using PLANE55 elements with different material properties according to the real situation. PLANE55 is a 2-D element with four nodes, and each node has a single degree of freedom (DOF) of temperature. It is endowed with thermal conduction capability and suitable for steady-state or transient thermal analysis.

The box-girder including the air in the inside hollow are entirely modeled to achieve a completely thermal equilibrium of the box-girder system, as shown in Fig. 3. The interaction of thermal radiation (thermal radiation boundary conditions) of the inside surface is calculated by AUX12 Radiation Matrix method using super-element MATRIX50. The thermal analysis FE of suspension cable and hanger are similar but with different size. The covering layers is modeled according to real situations. The spaces between parallel steel stranded wires are filled with air, it is difficult to model them separately. Therefore, the parallel steel stranded wires are simulated as homogeneous material with an equivalent material thermal parameters. The FE model of concrete tower column and cross beam for temperature analysis is also finely constructed, as shown in Fig. 3.

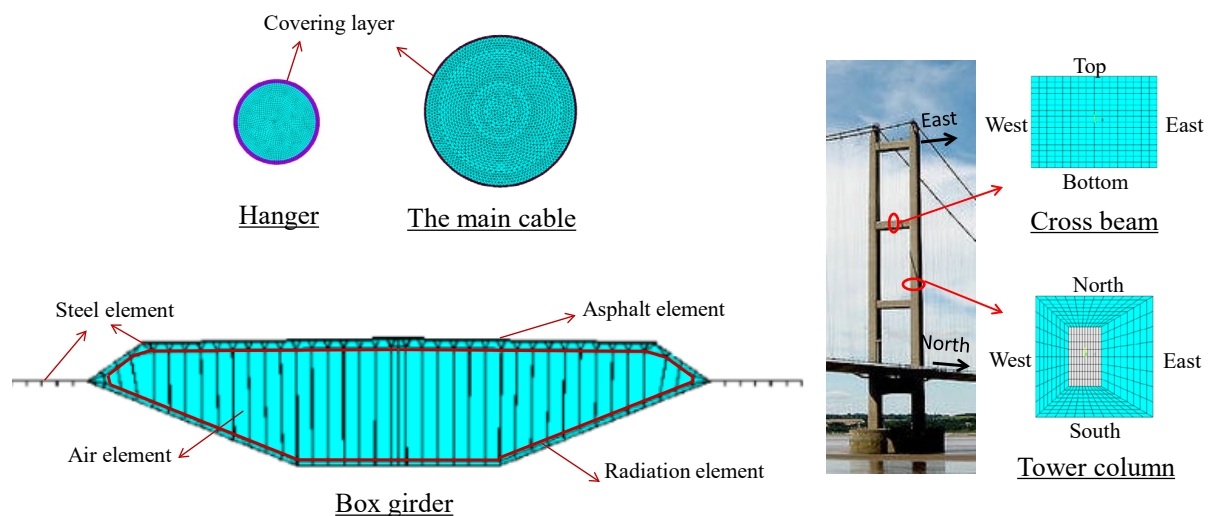


Fig. 3. The 2-D FE models for thermal analysis

### 3.2 FE model for structural analysis

The FE model of the suspension bridge for structural analysis is developed using 3-D model technology of ANSYS. The steel box-girder is modeled using SHELL181 elements. The pavement layer on the upper deck is only considered self-weight and ignore its contribution to stiffness. The concrete towers are constructed using SOLID65 elements. The suspension cables and hangers are modeled using LINK181 elements. At the end of the bridge girder, spring bearings are set up with COMBIN14 elements to simulate the real boundary conditions. The structural FE model and its details of the suspension bridge are illustrated in Fig. 4, which consisting a total of 117578 elements.

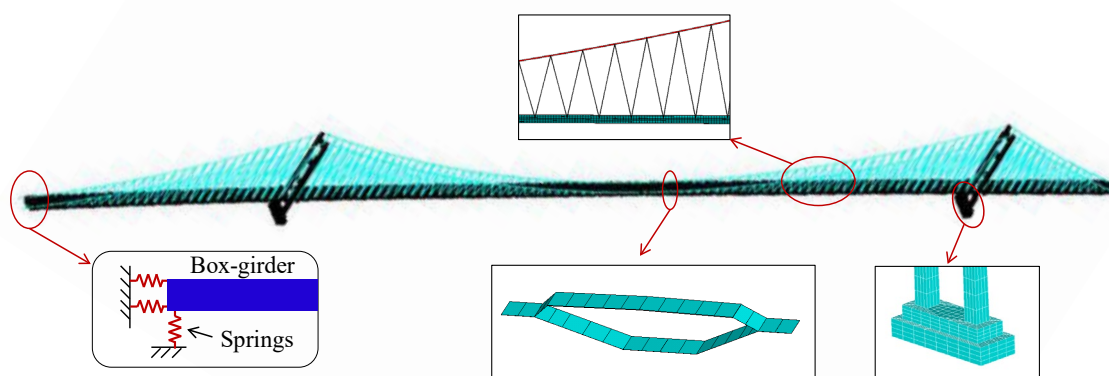


Fig. 4. The 3-D FE models for structural analysis

### 4. Thermal analysis of the suspension bridge

The energy exchanges between bridge and the surrounding environment consist of heat convection, heat conduction and thermal radiation. These processes highly depend on the outside environmental factors. To calculate the structural temperatures using FE method, one of the key issues is to properly determine the thermal boundary conditions. The authors of this study have carried out a comprehensive study on the numerical simulation of temperature for the box-girder of this suspension bridge (Zhou, et al., 2015). For brevity, the basic theory and method for calculation of thermal boundary conditions are not described here, which can be referenced to relative articles (Kehlbeck, 1975; Zhou, et al., 2015). The simulated temperatures of the box-girder can be found in the previous study (Zhou, et al., 2015). In this study, the temperatures of the other parts of this bridge at the same day (24 July, 2012) as the previous studies are calculated, and can then analyze the temperature-induced static response. The selected day, 24 July, 2012 is a typical sunny day with relative high solar radiation and air temperature.

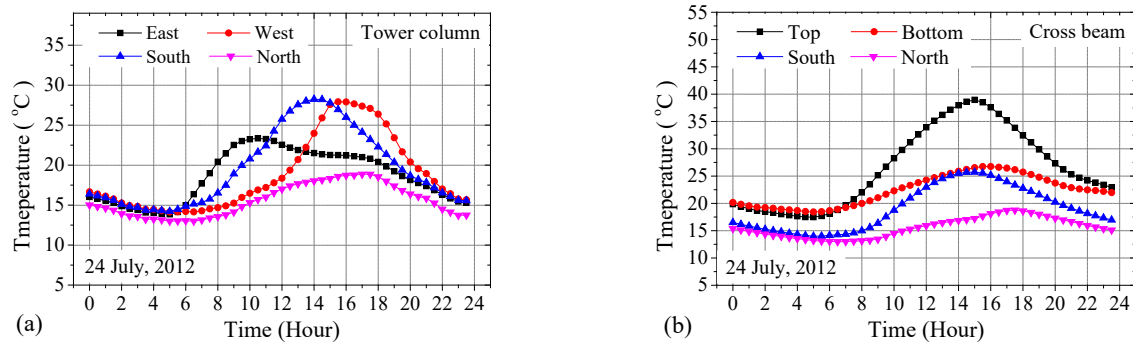


Fig. 5. Calculated temperatures of tower column and cross beam: (a) Tower column; (b) Cross beam

The calculated surface temperatures of the tower east column and cross beam are presented in Fig. 5. The temperature variations revealed good explanations of solar radiation effect on the structural surface. The east surface of tower column received higher level of solar radiation intensity than other surface in the morning, therefore it had a higher temperature and reached the maximum earlier. In the afternoon, west and south surface absorbed much solar radiation resulting of higher structural temperatures. The time of the maximum temperature of each tower column surface also indicated the sun moving from east to west in the daytime. The top surface of cross beam received much solar radiation, thus it had an obvious high temperature than other surfaces. The bottom surface had been shaded from the sun all day leading to the lowest temperature. As a conclusion, the validity of the heat transfer analysis of tower column and cross beam can be affirmed.

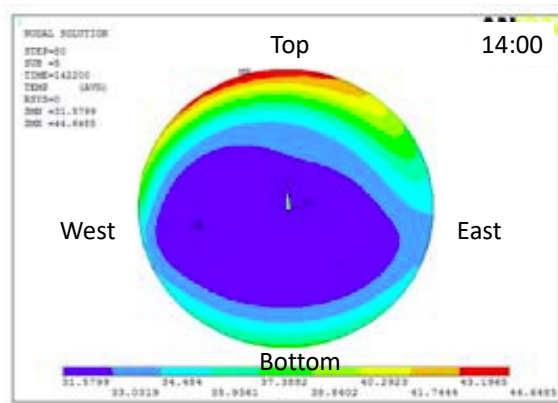


Fig. 6. Temperature field of main cable

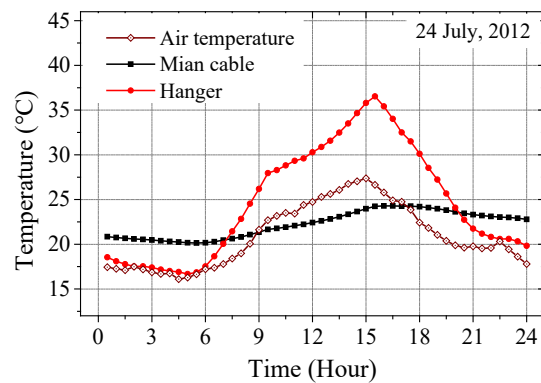


Fig. 7. Average temperatures of main cable and hanger

According to the variations of environmental factors, the thermal boundary conditions of main cable and hanger were calculated and then applied on the FE models, then transient thermal analysis was performed to obtain the temperatures. The temperature distribution of suspension cable at 14:40 is shown in Fig. 6. The top-west surface receiving more solar radiation resulted in higher temperature, and the energy was transferring from outside to inside



at this moment. The hanger's temperatures show the similar results. However, the cable and hanger are very slender with weak bending resistance, the temperature gradient of the section has very limited effects on their mechanical properties. Therefore, the average temperature was used for T-I structural responses analysis. The average temperature of main cable and hanger are shown in Fig.7. The hanger had obviously larger temperature and variation than main cable because the small size and thin covering layer make it more sensitive to the external environments such as air temperature and solar radiation.

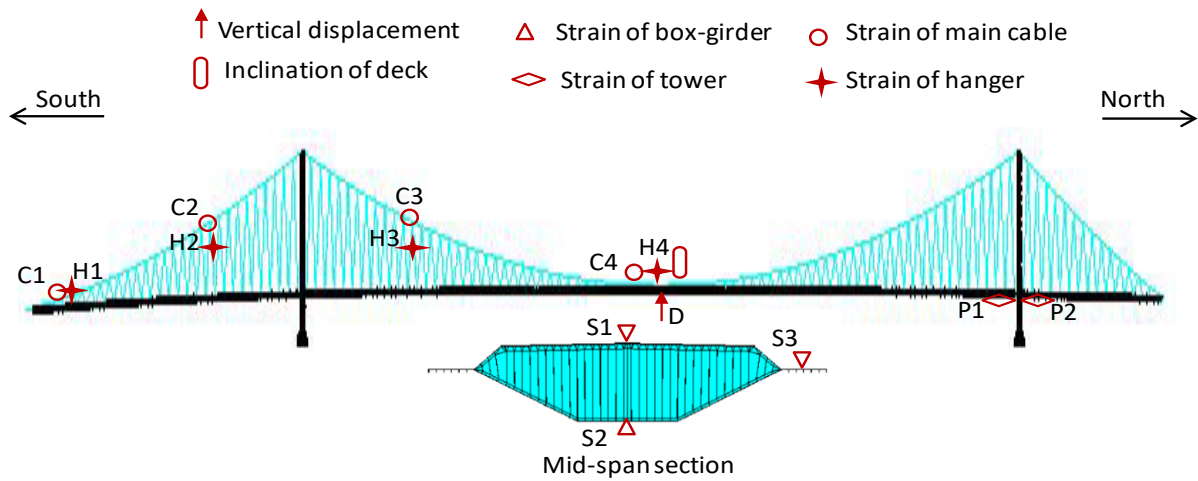


Fig. 8. Notations and locations of the discussed static responses

## 5. Structural static responses analysis

### 5.1 Static responses due to design vehicle load

In order to compare and assess the daily T-I static response of this suspension bridge, the static responses caused by design vehicle load is utilized for comparison. The discussed static responses of this suspension bridge are shown in Fig. 8. They are vertical displacement (D) and inclination (I) of bridge deck at the mid-span, strains of the mid-span box-girder section (S1-S3), strains of suspension cable at different points(C1-C4 ), strains of hanger at different points(H1-H4 ) and strains of the tower column near the bottom cross beam(P1 and P2 ). According to BS 5400, a uniformly distributed load of 17.3 kN/m was applied on each lane, meanwhile, a concentrated load of 120kN was applied at the mid-span. The static responses were calculated suing structural analysis of the structural FE model. The vehicle load-induced static responses of the concerned components are summarized in Tab.1 and Tab. 2.

Table 1. Static responses of box-girder section at mid-span due to design vehicle load

Parameters	Displacement (m)	Inclination(‰)	Strain ( $\mu\epsilon$ )		
Notation	D	C	S1	S2	S3

Value	4.03	0.01	17.9	28.9	0.4
-------	------	------	------	------	-----

Table 2. Strains of bridge components due to design vehicle load ( $\mu\epsilon$ )

Components	Main cable				Hanger				Tower	
Notation	C1	C2	C3	C4	H1	H2	H3	H4	P1	P2
Value	211.0	649.6	719.3	506.1	68.6	207.9	256.4	260.8	25.9	92.7

## 5.2 Temperature-induced static responses

The temperatures of the suspension bridge components on a typical sunny day (24 July, 2012) were obtained by numerical simulation using fine 2-D FE models, as described in Section 3. Then all the simulated temperatures are applied on the structural FE model to analyze the T-I static responses. The correspondingly node temperature is used for the box-girder and towers of structural FE model, and average temperatures are adopted for main cables and hangers. The structural analysis is carried out to obtain the T-I static responses such as displacement and strain.

### (1) T-I vertical displacement at mid-span

Selecting the start time (0:00) as reference, the variations of T-I vertical displacements at the mid-span are illustrated in Fig. 9. The calculated results showed very good agreement with the field measurements. Contrary to the temperature, the vertical displacement increased slightly and reached to the maximum around 05:00, then dropped to the minimum at about 16:00 then increased again. The total amount of diurnal change was about 0.5 meter. That was 12.4% of the vehicle response. The vertical displacements displayed reverse tendency with the structural temperatures. The bridge components expanded when the temperatures rising, especially for more slender components. Figure 10 shows the contribution of different components to the T-I vertical displacement, it can be seen the main cable and box-girder are the largest accounting for more than 90% of the displacement.

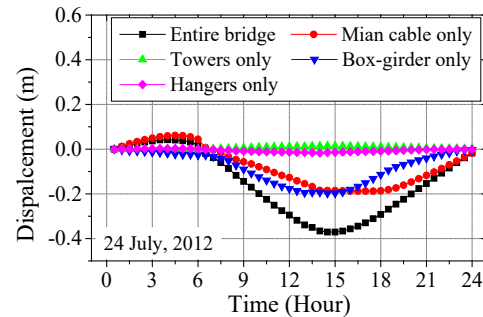
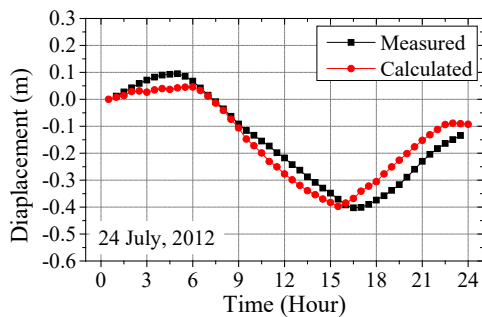


Fig. 9. T-I vertical displacement at the mid span

Fig. 10. Contribution of bridge components to the T-I  
vertical displacement

## (2) T-I lateral inclination at mid-span

The variations of lateral (east-west) inclinations of two days (24 July and 30 May, 2012) with different wind are calculated and discussed, as shown in Fig. 11. The simulated and measured results showed the similar tendency and indicated very high correlation with the transverse temperature difference (TTD) of box-girder. The inclinations synchronously varied with the changing of TTD. The inclination appeared positive value (the deck east side higher than west side) after the sunrise in the morning, that's because the east side of box-girder received more solar radiation resulting in higher temperature. Similarly, during the afternoon to sunset, the west side of box-girder had high temperature than the east side generating a negative value of inclination of the bridge deck. However, there were certain difference between the numerical and measured data because the environmental wind had significantly effects on the lateral inclinations of suspension bridge box girder. The average wind speed of 24 July and 30 May, 2012 were 3.9 m/s and 2.5 m/s, respectively. It can be seen that the numerical results of T-I inclination have better agreements with the measurements if the day with low wind speed.

For long-span suspension bridge, the deck inclination caused by temperature difference, wind and vehicle load, however, the vehicle load results in a transient inclination. Therefore, the diurnal variation of inclination mainly generated by temperature and wind. The total changes of measured inclination were 0.58 and 0.4 with respect to 24 July and 30 May, respectively. The corresponding T-I inclinations were 0.35 and 0.23, which were 60.34% and .57.5% of the measurements. It can be concluded that the TTD of box-girder is the major cause for the lateral inclination.

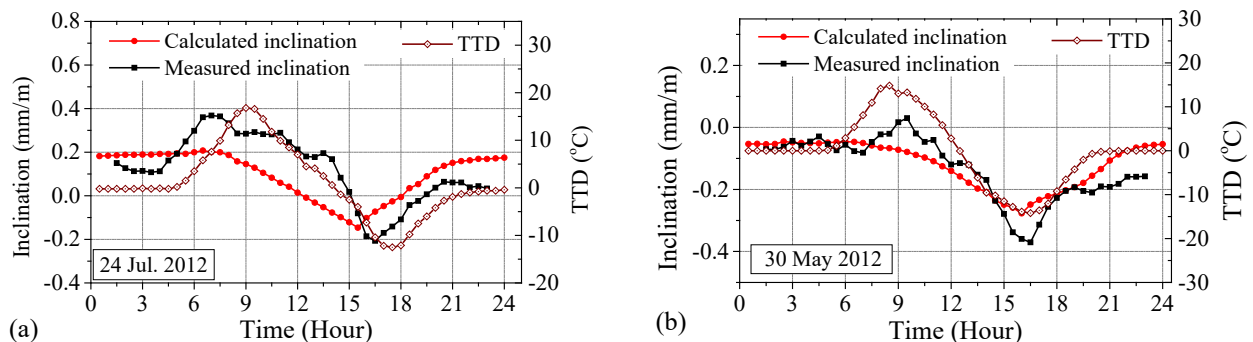


Fig. 11. Inclination and TTD of box-girder at the mid-span: (a) 24 July, 2012; (b) 30 May, 2012

## (3) T-I Strain of box-girder

The T-I strains and the average temperatures of box-girder section at the mid-span are shown in Fig. 12. The simulated

results exactly responded to the surrounding daily thermal environments. The structural temperature and strain decrease slightly and reached the minimum in the early morning, then increased dramatically to the maximum in the early afternoon, then dropped evidently during the evening to midnight. The variation of top (S1, S3) and bottom strains (S2) of the box-girder had opposite tendency since the temperature and its gradient made the box-girder bending. The increasing of temperature led to the top plate expanding and the bottom plate relative shrinkage. The variation amplitude of S1 and S2 this day were almost the same about  $150\mu\epsilon$ , they were dramatically larger than the strain caused by vehicle load, which were  $17.9\mu\epsilon$  and  $28.9\mu\epsilon$  for points S1 and S2, respectively. The box-girder flanges (S3) had the largest T-I strain with a total change of  $200\mu\epsilon$ , however, the strain of the box-girder flanges (S3) due to vehicle load was only  $0.4\mu\epsilon$ . The results convince us that the T-I strain is much larger than the vehicle load, even more for some secondary or accessory components.

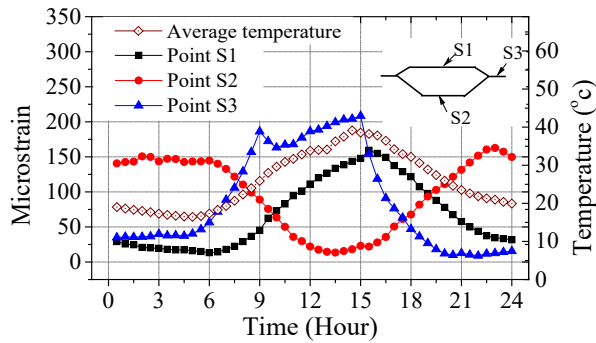


Fig. 12. Variation of the T-I strains and average temperature of box-girder (24 July, 2012)

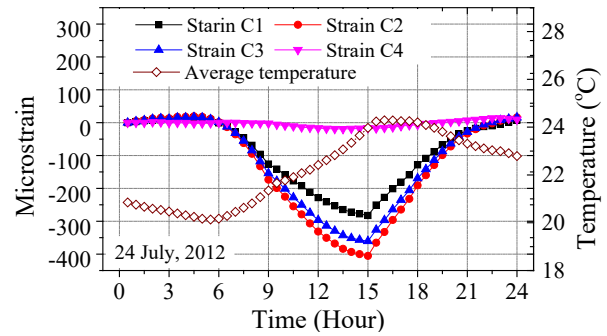


Fig. 13. Variations of the T-I strains and average temperatures of the main cable

#### (4) T-I strain of main cable

The temperature behavior of main cable deeply affect structural responses of the entire bridge, such as cable sag, tower deviation and box-girder deflection. The T-I strain and average temperatures of the main cable at four different positions (notated as C1 to C4, seen in Fig. 8) are extracted for discussion, as shown in Fig. 13. The T-I strain decreased with the increasing of temperature. The diurnal change of the four point T-I strain were  $47.6(C1)$ ,  $435.7(C2)$ ,  $471.9(C3)$  and  $331.9(C4)\mu\epsilon$ . They were sorted in descending order was C3, C2, C4 and C1, which was in accordance with the slope of main cable at these four locations, possible because the main cable segment with deeper slope was more sensitive to the vertical hanger actions. Comparing with the stains caused by design vehicle load as listed in Table 2., the changing amplitudes of T-I strain were  $22.6\%(C1)$ ,  $67.07\%(C2)$ ,  $65.61\%(C3)$  and  $65.58\%(C4)$  of the vehicle load.

## (5) T-I strain of hanger

Usually, the T-I strain of a single hanger significantly depends on its length and boundary condition. Longer length and stiffer boundary condition will lead to larger T-I strain. Four hangers (notated as C1 to C4, seen in Fig. 8) of the suspension bridge are selected to investigate the T-I strain. Taking the start time as reference point, the variations of the T-I strain on 24 July, 2012 are presented in Fig.14. All the T-I strains of the four hangers synchronous changed with the temperature, however, the changing amplitudes were different. The hanger H1 at the mid-span had the largest variation of  $225.5\mu\epsilon$ , however, the hanger H4 near the end of bridge, with similar length to H1, just had variation of  $73.295\mu\epsilon$ , that was because the hanger H1 with relative big dip angle at the mid-span had to resist more large displacement difference between suspension cable and bridge deck. Comparing with the stains of hanger caused by design vehicle load, the changing amplitudes of T-I strain were 86.46%(H1), 42.98%(H2), 28.28%(H3) and 106.84%(H4) of the vehicle load. Obviously, the temperature had larger negative effect on the short hanger than that of long hanger.

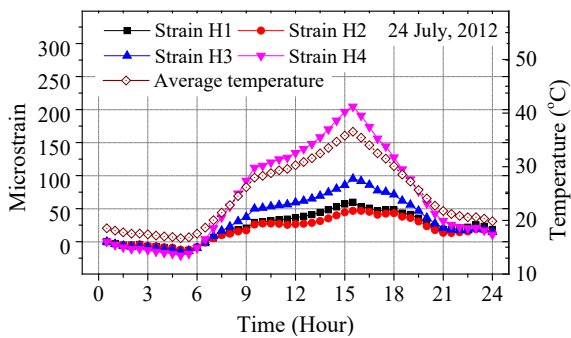


Fig. 14. T-I strain and average temperature of hangers

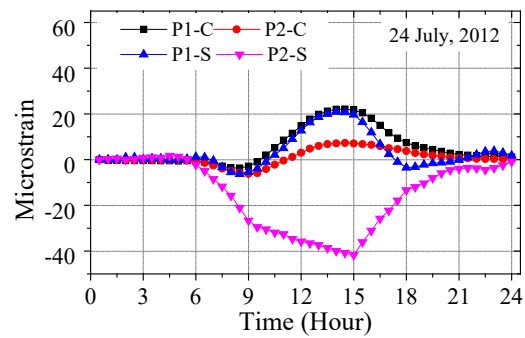


Fig. 15. T-I Strains of the tower at stage of construction and operation

## (6) T-I strain of tower

Towers of suspension bridge support the suspension cables, bear the entire loads of the bridge and deliver them to foundations. The height of hollow concrete towers of suspension bridge is always over hundreds meters. The temperatures effects of towers are essential for the construction and in-service stages of suspension bridge. However, the structural system and behavior of bridge tower under construction (without suspension cable) and operation stage are obviously different, therefore, the T-I strain of the two cases are simulated and discussed. Taking the start time as reference point, the strains extracted from the column surface points near the bottom cross beam are shown in Fig.15. The point P1 on the south side and P2 on the north side. Focusing on the case of construction stage, the T-I strain (P1-C and P2-C) had the same variation tendency synchronized with the changing of structural temperature. But the

south side (P1-C) had larger changing amplitude than the north side (P2-C) since the south side surface received more solar radiation on this day. Observing the strain at the operation stage (P1-S and P2-S), it is interesting to note that they had adverse variation during the daytime (8:30~18:00). The reason is that the temperature behavior are caused not only by the temperatures of tower itself, but also the temperatures effects of other components, especially the suspension cables. The strain of north-side point P2-S decreased with the temperature rising of whole bridge, because the suspension cables slacking made the tower top moving to the north, subsequently, the north side of tower column relatively compressed. Comparing with the stains of tower caused by design vehicle load, the changing amplitudes of T-I strain were 105.01% (P1) and 46.93% (P2) of the vehicle load, with an average of 75.97%. It can be seen the temperature effects are considerable.

## 6. Conclusions

Temperature effects are always the key issues for bridge especially large and long-span bridge. The temperature distribution and variation change the structural behavior has been widely recognized and verified by field monitoring. However, accurately analyzing the T-I structural behavior of long-span bridges is a challenge because of complex configuration and high uncertainties, and changing of meteorological environments. This paper carries out a deep and comprehensive investigation of T-I static responses based on a long-span steel box-girder suspension bridge. High-resolution FE models of this bridge for thermal analysis and structural analysis are constructed separately. Thermal boundary conditions are determined accounting for the real service environments, then performs the transient thermal analysis to obtain the time-dependent temperatures. Based on the structural FE model, the static responses caused by temperatures and design vehicle load are calculated and compared. The numerical results are also verified through a comparison with the field measurements. Based on the simulated and measured results of temperature effects based on this long-span steel box-girder suspension bridge, some conclusions are drawn as follows:

- 1) The change of T-I vertical displacement at the mid-span is about 0.45 meter, it is about 11.17% of the displacement caused by design vehicle load.
- 2) The inclination of bridge deck is mainly generated by TTD and the wind, the temperature takes account of up to 60% of the inclination for diurnal changes.
- 3) The box-girder has significant T-I strain with a day variation, which are several times larger than the strain caused by design vehicle load. The flanges of the box-girder has the largest T-I strain, however, the corresponding strain of design vehicle load is minimal to negligible. These may indicate that temperature

effects are the major load action for secondary structures of bridge.

- 4) The T-I strain of main cable highly depends on its slope, steeper cable is accompanied by larger T-I strain. The selected four points T-I strain are on average 66% of the strain caused by design vehicle load
- 5) The T-I strain of hanger is determined by its length and boundary conditions. The hanger at the mid-span has the largest T-I strain since its big dip angle and resisting more large displacement difference between suspension cable and bridge deck.
- 6) The T-I strain of tower column is caused not only by the temperatures of itself, but also the temperatures effects from main cables. The variation of T-I strain of the tower column near the bottom cross beam are on average of 75.97% of those caused by vehicle load.

Obviously, temperature effects on the static properties of long-span steel suspension bridge is remarkable. Some components T-I static responses even larger than the strain caused by design vehicle load. It worth noting that the structural temperatures used in this study are only one day data. Since the meteorological environments definitely have much larger variation in period of month, season and year, the temperature effects are sure to be even worse than this study. The temperature effects consume away a considerable part of the bearing capacity of bridge, meanwhile, they have strong time-varying characteristics and long-term effects. Therefore, temperature effects of long-span suspension bridge should be sufficiently considered in bridge design, and continuous monitoring and assessment in construction and operation stage.

## References

- [1] Priestley, M. (1976). "Design thermal gradients for concrete bridges." *New Zealand Engineering*, 31(9), 213-219.
- [2] Priestley, M. (1978). "Design of concrete bridges for temperature gradients." *ACI Journal Proceedings*, 75(5), 209-217.
- [3] Kennedy, J., Soliman, M. (1987). "Temperature distributions in composite bridges." *Journal of Structural Engineering*, 113(3), 65-78.
- [4] Salawu, O. S. (1997 ). " Detection of structural damage through changes in frequency: a review." *Engineering Structures* 19(9), 718-723.
- [5] Zuk, W. (1965). "Thermal behaviour of composite bridges -insulated and uninsulated." *Highway Research Record*, 76, 231-253.
- [6] Římal, J. (2001). "Measurement of Temperature Fields in Long Span Concrete Bridges." *Acta Polytechnica*, 41(6), 54-64.
- [7] Roberts-Wollman, C. L., Breen, J. E., and Cawrse, J. (2002). "Measurements of thermal gradients and their effects on segmental concrete bridge." *Journal of Bridge Engineering*, 7(3), 166-174.
- [8] Kromanis, R., and Kripakaran, P. (2017). "Data-driven approaches for measurement interpretation: analysing integrated thermal and vehicular response in bridge structural health monitoring." *Advanced Engineering Informatics*, 34, 46-59.
- [9] Zhou, G.-D., Yi, T.-H., Chen, B., and Chen, X. (2018). "Modeling deformation induced by thermal loading using long-term bridge monitoring data." *Journal of Performance of Constructed Facilities*, 32(3), 04018011.

- [10] Zhou, Y., and Sun, L. (2019). "A comprehensive study of the thermal response of a long-span cable-stayed bridge: From monitoring phenomena to underlying mechanisms." *Mechanical Systems and Signal Processing*, 124, 330-348.
- [11] Emerson, M. (1973). "The calculation of the distribution of temperature in bridges." Department of the Environment, TRRL Report LR 561, .
- [12] Kehlbeck, F. (1975). *Einfluss der Sonnenstrahlung bei Brückenbauwerken*, Werner - Verlag, Düsseldorf, West Germany (in German).
- [13] Hunt, B., Nigel, Cooke. (1975). "Thermal calculations for bridge design." *Journal of the Structural Division*, 101.ASCE# 11545 Proceeding.
- [14] Elbadry, M. M., Ghali, A. (1983). "Temperature variations in concrete bridges." *Journal of Structural Engineering*, 109(10), 2355-2374.
- [15] Tong, M., Tham, L.G., Au, F.T.K., Lee, P.K.K. (2001). "Numerical modelling for temperature distribution in steel bridges." *Computers & Structures*, 79(6), 583-593.
- [16] Xia, Y., Chen, B., Zhou, X. Q., Xu, Y. L. (2013). "Field monitoring and numerical analysis of Tsing Ma Suspension Bridge temperature behavior." *Structural Control and Health Monitoring*, 20(4), 560-575.
- [17] Zhou, L., Xia, Y., Brownjohn, J. M., and Koo, K. Y. (2015). "Temperature analysis of a long-span suspension bridge based on field monitoring and numerical simulation." *Journal of Bridge Engineering*, 21(1), 04015027.
- [18] Tayşi, N., and Abid, S. (2015). "Temperature distributions and variations in concrete box-girder bridges: Experimental and finite element parametric studies." *Advances in structural engineering*, 18(4), 469-486.
- [19] Zhu, J., and Meng, Q. (2017). "Effective and fine analysis for temperature effect of bridges in natural environments." *Journal of Bridge Engineering*, 22(6), 04017017.
- [20] Zhou, G.-D., and Yi, T.-H. (2013). "Thermal load in large-scale bridges: a state-of-the-art review." *International Journal of Distributed Sensor Networks*, 9(12), 217983.
- [21] Xu, Y., Chen, B., Ng, C., Wong, K., and Chan, W. (2010). "Monitoring temperature effect on a long suspension bridge." *Structural Control and Health Monitoring*, 17(6), 632-653.
- [22] Xia, Y., Chen, B., Zhou, X. q., and Xu, Y. I. (2013). "Field monitoring and numerical analysis of Tsing Ma Suspension Bridge temperature behavior." *Structural Control and Health Monitoring*, 20(4), 560-575.
- [23] Tomé, E. S., Pimentel, M., and Figueiras, J. (2018). "Structural response of a concrete cable-stayed bridge under thermal loads." *Engineering Structures*, 176, 652-672.
- [24] Yang, D.-H., Yi, T.-H., Li, H.-N., and Zhang, Y.-F. (2018). "Monitoring and analysis of thermal effect on tower displacement in cable-stayed bridge." *Measurement*, 115, 249-257.
- [25] Westgate, R., Koo, K.-Y., and Brownjohn, J. (2014). "Effect of solar radiation on suspension bridge performance." *Journal of Bridge Engineering*, 20(5), 04014077.
- [26] Reynolds, J. C. (1972). "Thermal stresses and movements in bridges."
- [27] Emerson, M. (1979). "Bridge temperatures for setting bearings and expansion joints." *Transportation Planning and Technology*, 5(Suppl Rpt. SR 479 Monograph).
- [28] Dilger, W. H., Ghali, A., Chan, M., Cheung, M. S., and Maes, M. A. (1983). "Temperature stresses in composite box girder bridges." *Journal of Structural Engineering*, 109(6), 1460-1478.
- [29] Mirambell, E., and Aguado, A. (1990). "Temperature and stress distributions in concrete box girder bridges." *Journal of Structural Engineering*, 116(9), 2388-2409.
- [30] Moorty, S., and Roeder, C. W. (1992). "Temperature-dependent bridge movements." *Journal of Structural Engineering*, 118(4), 1090-1105.
- [31] Fujino, Y., Murata, M., Okano, S., and Takeguchi, M. "Monitoring system of the Akashi Kaikyo Bridge and displacement measurement using GPS." *Proc., SPIE*, International Society for Optics and Photonics, 229-236.
- [32] Yang, D., Youliang, D., and Aiqun, L. (2010). "Structural condition assessment of long-span suspension bridges using



long-term monitoring data." *Earthquake Engineering and Engineering Vibration*, 9(1), 123-131.

[33] Kromanis, R., Kripakaran, P., and Harvey, B. (2016). "Long-term structural health monitoring of the Cleddau bridge: evaluation of quasi-static temperature effects on bearing movements." *Structure and Infrastructure Engineering*, 12(10), 1342-1355.

[34] Roeder, C. W. (2003). "Proposed design method for thermal bridge movements." *Journal of Bridge Engineering*, 8(1), 12-19.

[35] Ni, Y., Hua, X., Wong, K., and Ko, J. (2007). "Assessment of bridge expansion joints using long-term displacement and temperature measurement." *Journal of Performance of Constructed Facilities*, 21(2), 143-151.

[36] Duan, Y.-F., Li, Y., and Xiang, Y.-Q. "Strain-temperature correlation analysis of a tied arch bridge using monitoring data." *Proc., 2011 International Conference on Multimedia Technology*, IEEE, 6025-6028.

[37] Wang, G.-X., Ding, Y.-L., Sun, P., Wu, L.-L., and Yue, Q. (2015). "Assessing static performance of the Dashengguan Yangtze Bridge by monitoring the correlation between temperature field and its static strains." *Mathematical Problems in Engineering*, 2015.

[38] Xia, Q., Cheng, Y., Zhang, J., and Zhu, F. (2016). "In-service condition assessment of a long-span suspension bridge using temperature-induced strain data." *Journal of Bridge Engineering*, 22(3), 04016124.

[39] Hyder, C. (2007). "Footprints on a Global Landscape (150 Years of Improving the Built Environment)." *UK: Gordon Hunt Design*.

[40] Fisher, D. (1982). "Design and Construction of The Humber Bridge." *The Institute of Physics*.